

Fabrication and bioactivity evaluation of curcumin and paclitaxel loaded lipid nanoparticles of pH-sensitive histidinylated cationic amphiphile

Swathi Vangala^{1,2}, Gopikrishna Moku^{1,3}

Cite this article: Vangala S, Moku G: Fabrication and bioactivity evaluation of curcumin and paclitaxel loaded lipid nanoparticles of pH-sensitive histidinylated cationic amphiphile. *Asia-Pac J Oncol* 2021; 2: 7-16. <https://doi.org/10.32948/ajo.2021.04.06>

Abstract

Drug resistance, inefficient cellular uptake and the subservient drug release to increase the intracellular drug concentration inside the tumor cells are the key reasons for low therapeutic efficacy of drug-loaded lipid nanoparticles in cancer therapy. Herein, we report on the design, synthesis and bioactivity evaluation of Curcumin & Paclitaxel (PTX) encapsulated endosomal pH-Sensitive lipid nanoparticles of histidinylated cationic amphiphile (16-GH; 2 in 1 system) to overcome these challenges. Findings in fluorescence resonance energy transfer (FRET) assay and in vitro drug release studies showed a controlled pH dependent fusogenic and drug release properties of the lipid nanoparticles of cationic amphiphile 16-GH respectively. Further in vitro studies revealed that Curcumin & PTX encapsulated nanoparticles of lipid 16-GH significantly inhibited proliferation of tumor cells than healthy cells. These lipid nanoparticles were further analyzed for their effect on 5-bromo-2'-deoxyuridine (BrdU) incorporation, Annexin V-FITC and cell cycle arrest (Sub-G1 phase). Further studies also confirmed that nanoparticles of lipid 16-GH containing Curcumin & PTX displayed significantly enhanced the caspase3/9 activity. Remarkably, nanoparticles of lipid 16-GH containing Curcumin & PTX are efficient in inducing apoptosis. The results in our initial mechanistic studies support the notion that the tumor cell selective cytotoxic capability of the lipid nanoparticles of the presently described endosomal pH-sensitive lipid probably instigates from depolarization of mitochondrial membrane potential and subsequent activation of caspases 3 and 9. The distinguishing feature of the currently described endosomal pH-sensitive system is that it not only efficiently delivers highly potent anti-cancer agents (Curcumin & PTX) to tumor cells, but the lipid nanoparticle drug carrier itself also contributes to inhibiting tumor cell growth. In summary, the presently described lipid nanoparticles are expected to simultaneously delivering combination of drugs to various types of tumor models.

Key words Endosomal pH-sensitivity, histidinylated cationic amphiphiles, Curcumin, paclitaxel, fusogenic lipid nanoparticles, intra cellular drug delivery

1. Applied Biology Division, CSIR-Indian Institute of Chemical Technology (CSIR-IICT), Tarnaka, Uppal Road, Hyderabad 500 007, India.

2. Telangana Social Welfare Residential Degree College for Women, Bhupalapally 506 169, Telangana, India.

3. Department of Physical Sciences, Kakatiya Institute of Technology and Science, Yerragattu Gutta, Warangal 506 015, Telangana, India

Correspondence: Gopikrishna Moku (Department of Physical Sciences, Kakatiya Institute of Technology and Science, Yerragattu Gutta, Warangal 506 015, Telangana, India; Email: gopikrishna.moku@gmail.com; mgkr.pss@kitsw.ac.in).

Introduction

In recent years, several controlled drug-delivery technologies [1-5] have been employed to increasing the intracellular anti-neoplastic drugs concentration in cancer cells. Drug vehicles, i.e. micelles [6, 7], lipid nanoparticles [8, 9], peptides [10], polymers [11, 12] and inorganic nanoparticles [13, 14] that are sensitive to tumor acidic pH are gaining importance for efficient release into tumor cells. pH-Sensitive lipid nanoparticles have been extensively studied in recent years as an important alternative to conventional lipid nanoparticles in effectively delivering and accumulating anti-cancer drugs in tumor cells due to their fusogenic property. During cationic mediated drug delivery, drugs encapsulated lipid nanoparticles enter cells usually by endocytotic pathway, following internalization, the endocytosed lipid nanoparticles fuses with endosomes. The ATPase in the endosomal membrane causes an influx of protons which results in a continuous pH drop as endosomes mature from early endosomes to late endosomes. If the drugs cannot promptly escape from endosomes, the acidic environment of lysosomes might activate the lysosomal enzymes for the degradation of the released drug [16]. Therefore, the intracellular pH-sensitive moieties with the ability to destabilize the endosomal membrane or rupture the endosomes can be used to modify lipid nanoparticles that facilitate endosomal escapement. In addition, the use of drug-loaded lipid nanoparticles that destabilizes at an early endosomal pH of 6.0 should maximize intracellular drug delivery and minimize drug release at the extracellular pH and at the lysosomal pH [17]. Two decades back Wolff and co-workers pioneered the use of cationic lipids containing endosomal pH-sensitive (pH 5.5-6.5) imidazole head-groups [18]. The pKa of the weakly basic imidazole head-groups being within the acidity range of endosomal lumen (pH 5.5-6.5), the imidazole head-groups act as a proton sponge while inside the endosome compartments. Such endosomal buffering induces stronger electrostatic repulsion among the protonated imidazole head-groups leading to osmotic swelling and eventually bursting of the endosomes due to entry of lots of hydrated chloride counter ions [19]. Therefore drug encapsulated pH-sensitive imidazole group containing lipid nanoparticles are believed to increase the efficiency of targeting drugs to desired cellular sites while effectively protecting them from being potentially degraded at the endosomal level.

To this end, recently we reported cancer cell selective cytotoxicities, as well as tumor growth inhibition properties of endosomal pH-sensitive lipid nanoparticles of histidinylated cationic lipids [20]. However, as described below, these cationic amphiphiles with pH-sensitive histidine head-group failed to show serum stability and therapeutic efficiencies when administered

(16-GH+Cur+PTX) were so efficient in killing cancerous cells compared to untreated cells.

Materials and Methods

General Methods and Reagents

Paclitaxel, Curcumin, 3-(4,5-Dimethylthiazol-2-yl)-2,5-diphenyltetrazolium bromide (MTT), Propidium Iodide (PI), FITC labeled Annexin V, cell culture media, fetal bovine serum, Trizol reagent, dimethylsulfoxide (DMSO), agarose, cholesterol, HEPES, DOPC and cell culture lysis buffer were purchased from Sigma-Aldrich, USA. DSPE-(PEG)₂₇-NH₂ was purchased from Avanti Polar Lipids, USA. All the other reagents were purchased from local suppliers and used without further purification. A549, MCF-7, CT26, B16F10, COS-1 and NIH3T3 were purchased from the National Centre for Cell Sciences, NCCS, Pune, India. Cells were grown at 37 °C in DMEM/RPMI-1640 containing 10% FBS in a humidified atmosphere containing 5% CO₂.

Preparation of lipid nanoparticles

Lipid nanoparticles were prepared following previously published protocol [20]. pH-Sensitive cationic lipid 16-GH, DOPE, cholesterol and DSPE-(PEG)₂₇-NH₂ at 1:1:0.5:0.05 mole ratios were dissolved in a mixture of chloroform and methanol (3:1, v/v) in a glass vial. Curcumin and PTX stock solutions were prepared by dissolving in a mixture of chloroform and methanol (3:1, v/v) in a vial. The final total lipid 16-GH: Curcumin ratio (w/w) used in preparing the nanoparticles of lipid 16-GH containing only Curcumin (16-GH+Cur) and nanoparticles of lipid 16-GH containing both Curcumin & PTX (16-GH+Cur+PTX) was 10:1 for both in vitro and in vivo experiments. 8.5 µg of PTX was used in lipid nanoparticles for in vitro experiments. The solvents were removed with a thin flow of moisture free nitrogen gas, kept under high vacuum for 8 h, 1 mL sterile deionized water was added to the vacuum dried lipid films and allowed to swell overnight. The vials were then vortexed for 3-4 min at room temperature to produce multilamellar lipid vesicles (MLVs), sonicated in an ice bath until clarity using a Branson 450 sonifier at 100% duty cycle and 25W output power to produce small unilamellar vesicles (SUVs). Curcumin, PTX and Curcumin & PTX encapsulated lipid nanoparticles were finally centrifuged for 45 min at 5000 × g to remove unencapsulated Curcumin and PTX. The amount of Curcumin and PTX were determined spectrophotometrically at a wavelength of 450 nm and 230 nm respectively.

The drug encapsulation efficiencies were calculated as follows:

$$\text{Entrapment efficiency (\%)} = \frac{\text{Weight of entrapped drug in lipid nanoparticles}}{\text{Weight of the drug used}} * 100$$

intravenously. In addition, these lipid nanoparticles IC₅₀ values were found to be 15-20 µM [20]. Further, to increase the anti-proliferative efficiency of most potent lipid nanoparticles of a novel cationic amphiphile containing glutamic acid and endosomal pH-sensitive histidine head-group and two n-hexadecyl hydrophobic tails (in short form 16-GH) [20], in the present study we encapsulated two hydrophobic anti-cancer agents Curcumin and Paclitaxel (PTX) in its counter parts. Findings in in vitro MTT assay studies in cancerous cells, demonstrated that lipid nanoparticles of 16-GH containing both PTX and Curcumin

Zeta potential (ζ) and size measurements

Photon correlation spectroscopy and electrophoretic mobility on a Zeta sizer 3000HSA (Malvern UK) were used to measure the sizes and the global surface charges (zeta potentials) of nanoparticles of lipid 16-GH, 16-GH+Cur, 16-GH+PTX, and 16-GH+Cur+PTX. The sizes were measured in deionized water with a sample refractive index of 1.59 and a viscosity of 0.89. Polystyrene beads (Duke Scientific Corps. Palo Alto, CA) in the range of 200 ± 5 nm

were used to calibrate the system. Automatic mode was used to calculate the hydrodynamic diameters of the lipid nanoparticles. Viscosity, 0.89 mPa·s; dielectric constant, 79; temperature, 25 °C; F(Ka), 1.50 (Smoluchowski); maximum voltage of the current, V parameters were used to measure the zeta potential. DTS0050 standard from Malvern, UK was used to calibrate the system. Measurements were done 10 times with the zero-field correction. The potentials were calculated by using the Smoluchowski approximation.

FRET Assay

FRET assay was used to measure the pH-dependent membrane fusion activity of the lipid nanoparticles of 16-GH as described previously [21]. The bio membrane mimicking lipid nanoparticles containing DOPC/DOPE/DOPS/Chol at 45:20:20:15, w/w ratio, with the total lipid concentration of 0.5 mM, were labeled with the donor (0.005 mM NBD-PE, Avanti-Polar Lipids, USA) and acceptor lipids (0.005 mM Rho-PE, Avanti-Polar Lipids, USA). The total lipid concentration in the nanoparticles of lipid 16-GH was also kept at 0.5 mM. At pH 7.4, 6 and 5, equimolar amounts of the lipid nanoparticles were mixed with labeled model bio membrane lipid nanoparticles in an FLX 800 Microplate Fluorescence Reader (BioTek Instruments Inc., U.K.) at room temperature and the fluorescence intensities were recorded as a function of time using 485 nm excitation wavelength and 595 nm emission wavelength. 1% Triton X100 was used to measure 100% fusion from the Rho-PE fluorescence intensity observed for

$$\text{Percent viability} = \frac{A570(\text{treated cells}) - \text{background}}{A570(\text{untreated cells}) - \text{background}} * 100$$

labeled bio membrane lipid nanoparticles.

In vitro drug release studies

In vitro drug release profile of lipid nanoparticles of 16-GH+Cur and lipid nanoparticles of 16-GH+PTX was done by direct dispersion method as described previously [22]. In vitro drug release studies were done at pH 7.4, 6.0 and 5.0. Briefly, lipid nanoparticles containing a known quantity of Curcumin and PTX were sub-divided into several equal volume parts in different Eppendorf tubes, each part was diluted with buffers of different pH values and the mixed solutions were incubated in a water bath shaker at 37 °C. At definite time intervals, tubes were taken out and centrifuged at 1200 × g for 3 min. The pellets were dissolved in 0.5 mL ethanol and the amounts of Curcumin & PTX released were quantified spectrophotometrically at a wavelength of 450 nm & 228 nm respectively.

Cell Culture

A549, B16F10, C26, MCF7, COS-1 and NIH3T3 cells (Mycoplasma free) were procured from National Center for Cell Sciences (Pune, India). Cells were cultured at 37 °C in a humidified atmosphere of 5% CO₂ in air in DMEM/RPMI-1640 medium (Sigma) containing 10% fetal bovine serum (South American Origin, Gibco, USA) and 1% penicillin-streptomycin-kanamycin. For all in vitro and in vivo experiments, 75-80% confluent cultures of cells were used.

Cellular uptake studies

CT-26 (~2 × 10⁵ cells per well) were cultured onto six-well plates. After 24 h of incubation, Rho-PE (0.1 mol% with respect to lipid 16-GH) labelled nanoparticles of lipid 16-GH, 16-GH+Cur, 16-GH+PTX, 16-GH+Cur+PTX were added. After 2 h, cells were trypsinized, centrifuged at 2000 × g for 3 min, cell pellet was washed with PBS (500 μL) and resuspended in PBS (500 μL). The cellular uptake of Rho-PE labelled lipid nanoparticles, were measured with a flow cytometer (FACS Canto II, BD).

In vitro cell growth inhibition studies

Growth inhibition of cancer cells and non-cancer cells by the nanoparticles of lipid 16-GH, 16-GH+Cur, 16-GH+PTX, 16-GH+Cur+PTX were evaluated by the 3-(4,5-dimethylthiazol-2-yl)-2, 5-diphenyltetrazolium bromide (MTT) reduction assay. A549, MCF7, B16F10, CT26, COS-1, and NIH3T3 cells were seeded at a density of ~10,000 cells per well in 96-well plates, incubated for 18-24 h. Cells were treated with various concentrations of lipid nanoparticles using DMEM/RPMI-1640 medium (Sigma) containing 10% fetal bovine serum. After 24 h, 10 μL of MTT solution (5 mg/mL in PBS) was added to the cells and incubated for 4 h. MTT is reduced to formazan (purple color) by living cells but not by dead cells. The formazan crystals were dissolved with 50 μL of 1:1 (v/v) DMSO/Methanol. Absorbances of the wells were determined with a microplate reader (ELISA) at 550 nm wavelength. Results were expressed as

The percent of cell growth inhibition was calculated with reference to the control values (without the addition of any lipid nanoparticles). The data were subjected to linear regression analysis, and the regression lines were plotted for the best straight-line fit. The IC₅₀ (inhibition of cell growth) concentrations were calculated using the respective regression equation.

Flow Cytometric apoptosis analysis

At a density of ~3 × 10⁵ cells per well, CT-26 and NIH3T3 cells were seeded in 6 well plates. After 18-24 h, medium was replaced with 1.5 mL DMEM medium containing 10% FBS, followed by addition of nanoparticles containing 15 μM lipid 16-GH without any drug, nanoparticles containing 15 μM lipid 16-GH & 10 μM Curcumin; nanoparticles containing 15 μM lipid 16-GH & 20 nM PTX; and nanoparticles containing 10 μM lipid 16-GH & 5 μM Curcumin & 10 nM PTX. After 24 h incubation, cells were trypsinized, centrifuged at 2000 × g for 3 min and cell pellets were resuspended in 500 μL binding buffer containing 5 μL of annexin-V FITC and 10 μL of PI. The mixture was incubated for 15 min in dark and analyzed by flow cytometer (BD FACS Canto II).

BrdU incorporation assay

CT-26 and NIH3T3 cells were seeded at a density of ~20,000 per well in a 96-well plate. After 18-24 h, cells were treated with nanoparticles containing 15 μM lipid 16-GH without any drug, nanoparticles containing 15 μM lipid 16-GH & 10 μM Curcumin;

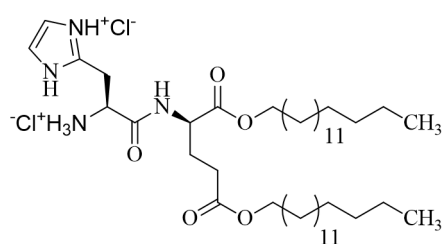


Figure 1. The structures of the endosomal pH-sensitive histidinylated cationic lipid 16-GH used in the preparation of various lipid nanoparticles.

nanoparticles containing 15 μM lipid 16-GH & 20 nM PTX; and nanoparticles containing 10 μM lipid 16-GH & 5 μM Curcumin & 10 nM PTX. After 24 h of incubation, the medium was discarded and 100 μL 10% complete medium containing 20 μL of 1 \times BrdU reagent was added to each well. BrdU incorporation assay was then performed by using BrdU Cell Proliferation Assay Kit (Millipore) as per manufacturer's instructions.

Flow cytometric cell cycle analysis

CT-26 cells were grown in the presence of 2 mM thymidine (Sigma) for 18 h, washed with PBS, sub cultured and grown in fresh medium without thymidine for 8 h. Cells were then incubated with 2mM thymidine for 18 h to block cells at the G1/S boundary and then grown in fresh medium for 2. The cells ($\sim 1 \times 10^6$ cells per flask) were treated with one of the following: nanoparticles containing 15 μM lipid 16-GH without any drug, nanoparticles containing 15 μM lipid 16-GH & 10 μM Curcumin; nanoparticles containing 15 μM lipid 16-GH & 20 nM PTX; and nanoparticles containing 10 μM lipid 16-GH & 5 μM Curcumin & 10 nM PTX in 4 mL complete medium. After 24 h, cells were detached from the flask by trypsinization, fixed by 2% paraformaldehyde in PBS, permeabilized by 0.1% Triton-X 100 in PBS and pelleted. 1 mg of primary antibody to Cyclin B1 (a marker of G2/M phase of cell cycle) in 250 μL of PBS was added to the cell pellets followed

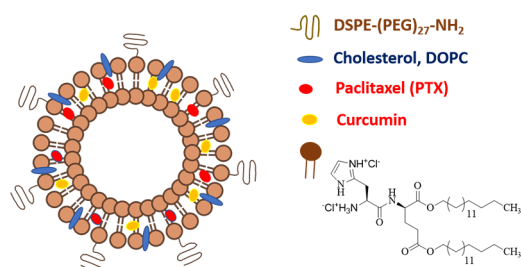


Figure 2. pH-Sensitive lipid nanoparticles of cationic amphiphile 16-GH containing co-solubilized PTX and Curcumin.

by vortexing and incubation for 30 min in a covered ice-bucket. Supernatant was aspirated and 250 μL of PBS was added to each pellet, 1 mg of (FITC)-conjugated secondary antibody was added, followed by vortexing and incubation for 30 min in a covered ice-bucket. Supernatant was discarded and the pellets were resuspended in PBS (500 μL) and analyzed by flow cytometry (BD FACS Canto II).

Statistical analysis

The statistical significance of the experiments was determined by two-tailed Student's test. *P < 0.05 were considered statistically significant. Error bars represent mean values \pm SEM.

Results and Discussion

Chemistry

The histidinylated cationic lipid 16-GH (**Figure 1**) was synthesized by following our previously published protocol [20]. This lipopeptide was confirmed by 1H-NMR spectroscopy and mass spectrometry.

Sizes and Zeta potentials (ξ) of the lipid nanoparticles

Table 1. Sizes and Zeta potentials (ξ) of various lipid nanoparticles used in the present study.

Lipid nanoparticles containing	Hydrodynamic diameters (nm)	Zeta Potentials (mV)	Curcumin entrapment efficiencies (%)	Paclitaxel entrapment efficiencies (%)
Lipid 16-GH	135 \pm 2.1	2.2 \pm 1.1	NA	NA
Lipid 16-GH & Curcumin	169.7 \pm 3.5	3.9 \pm 0.5	91.1 \pm 4.7	NA
Lipid 16-GH & PTX	189.4 \pm 1.8	3.1 \pm 0.9	NA	97.4 \pm 1.1%
Lipid 16-GH, Curcumin & PTX	205.8 \pm 2.2	2.1 \pm 0.1	90.2 \pm 3.5	96.3 \pm 1.9%

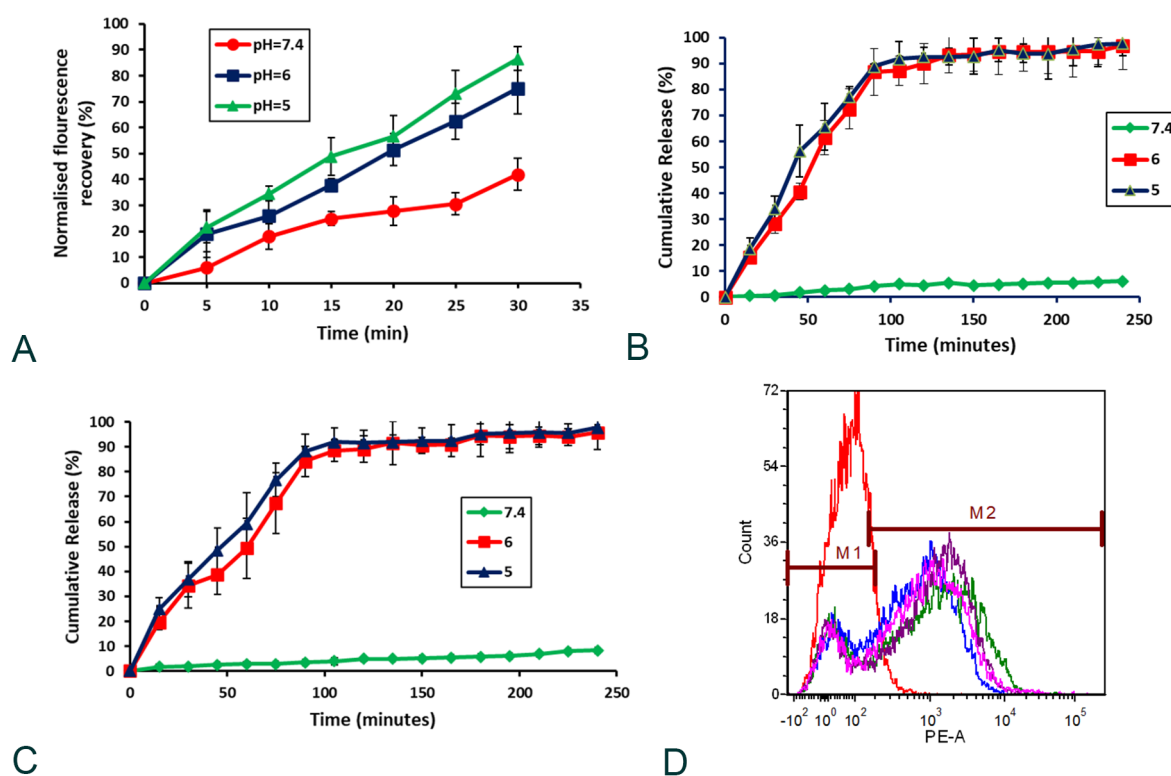


Figure 3. (a) The membrane fusion activity of nanoparticles of lipid 16-GH. Fusion versus pH. Drug release profile of Curcumin from lipid nanoparticles containing Curcumin (b) & paclitaxel (c) in three different pHs 5, 6 and 7.4. Cellular uptake quantification of Rh-PE (red) labeled lipid nanoparticles containing only 16-GH (blue); lipid nanoparticles containing 16-GH+Curcumin (pink); lipid nanoparticles containing 16-GH+PTX (green); lipid nanoparticles containing 16-GH+Curcumin+PTX (violet); control (red) by flow cytometry in CT-26 (d) after 2 h of incubation.

Hydrodynamic diameters (zeta sizes) and the global surface charges (zeta potentials) of the lipid nanoparticles (Figure 2) measured by dynamic light scattering technique were found to be within the range of 135-205 nm and 2-4 mV (Table 1). The drug entrapment efficiencies for Curcumin & PTX were shown in Table 1. The entrapment efficiency of Curcumin (~91%) in nanoparticles of lipid 16-GH+Cur was found to be similar compared with Curcumin in nanoparticles of lipid 16-GH+Cur+PTX (~90%).

FRET assay, in vitro drug release and cellular uptake studies

First, we performed the Fluorescence resonance energy transfer (FRET) assay to confirm the endosomal pH-sensitivity of the presently described nanoparticles of histidinylated cationic lipid 16-GH by measuring the biomembrane fusibility. FRET experiments carried out at pH 5 & 6 (i.e. near the endosomal pH range) significantly enhanced fusion of the nanoparticles of lipid 16-GH with the biomembrane mimetic lipid nanoparticles compared at pH 7.4 (Figure 3a). Results clearly demonstrated the endosomal pH-sensitivity of the nanoparticles of lipid 16-GH. Next, we evaluated, the in vitro drug release studies via the direct dispersion method at pH 5, 6 and 7.4 and the release pattern is shown in Figure 3b. Findings in in vitro drug release studies clearly demonstrated that the lipid nanoparticles were found to be highly stable at pH 7.4. At pH 5 and 6, Curcumin and PTX was released from the lipid nanoparticles in a pH-dependent and time-dependent manner, 90% of the drug released from the lipid nanoparticles after 2 h of incubation (Figure 3b). The drug

release pattern showed a burst release in the first 1 h followed by a controlled release of Curcumin & PTX over a period 4 h and about 85% of drug was released during this time. Protonation of the imidazole -N-H at pH 5 and 6 might be increasing the repulsions between the adjacent protonated imidazole group causing the release of Curcumin and PTX from the lipid nanoparticles. These findings support the notion that the endosomal pH-sensitivity of the presently described lipid nanoparticles.

In vitro cell uptake studies of lipid nanoparticles of 16-GH, 16-GH+Cur, 16-GH+PTX, and 16-GH+Cur+PTX in CT-26 were done by flow cytometry to check the cancer cell selectivity of the lipid nanoparticles. The lipid nanoparticles were labeled with Rh-PE (red), quantified the uptake by flow cytometry method was shown in Figure 3c. The significant cellular accumulation of lipid nanoparticles was observed in CT-26 cells after 2 h of incubation (Figure 3c).

In vitro cell growth inhibition study

MTT assay was conducted to examine the cellular cytotoxicity profiles of the various lipid nanoparticles in inhibiting growth of cancer cells including human breast (MCF-7), lung (A549), pancreatic cancer (CT-26), mouse melanoma (B16F10), and healthy mouse fibroblast (NIH-3T3), African Green Monkey Kidney (COS-1) cells. The cells were subjected to varying doses of drugs encapsulated in lipid nanoparticles. The findings in the MTT assay convincingly demonstrated that lipid nanoparticles were effectively killing cancer cells (Figure 4a-d). Importantly, slight

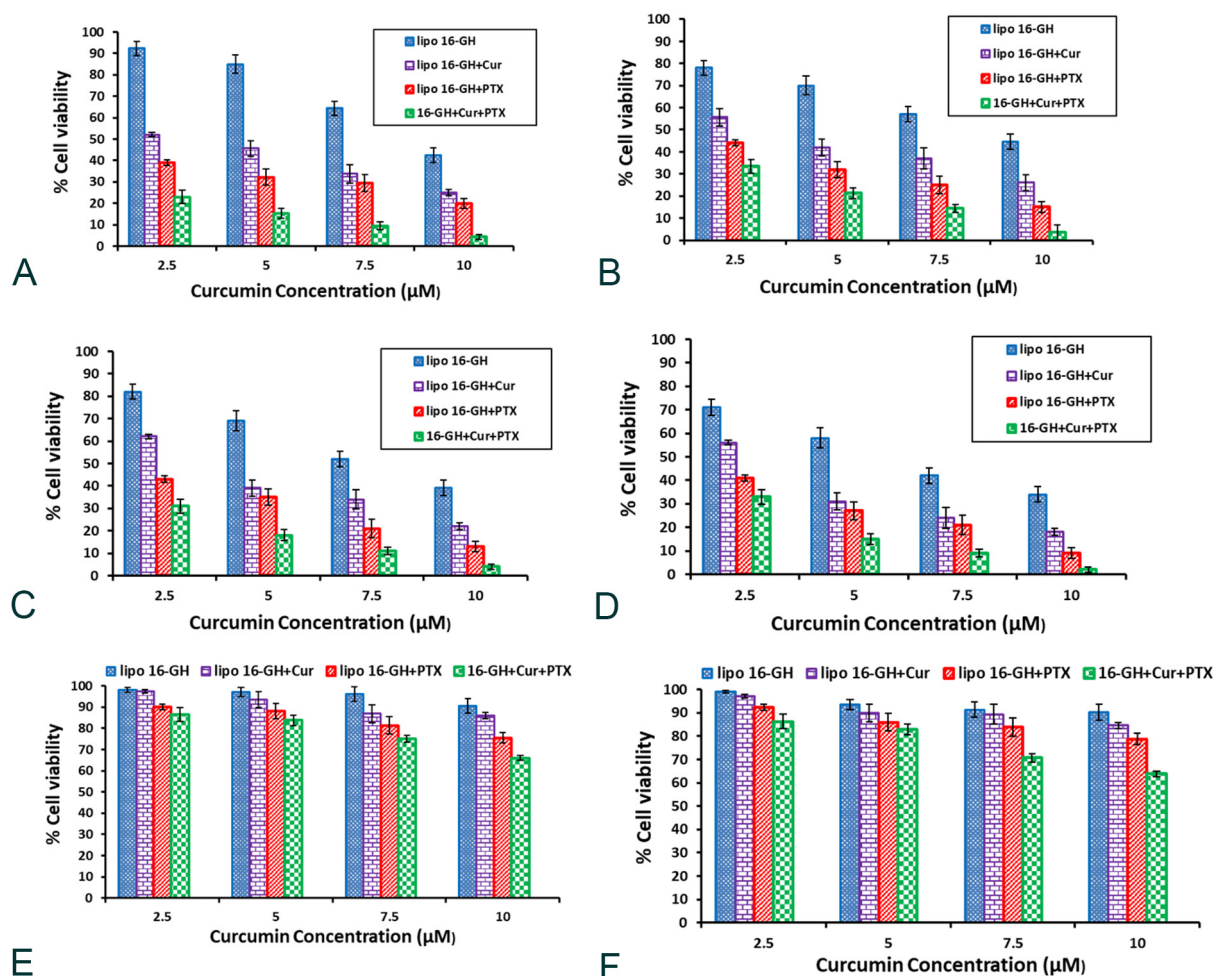


Figure 4. Curcumin and PTX co-encapsulated nanoparticles of lipid 16-GH show significant cytotoxicity in cancerous (A549 (a), B16F10 (b), MCF 7 (c) & CT26 (d)) cells and slight cytotoxicity in non-cancerous cells (COS-1 (e) & NIH3T3 (f)). Cells were treated with nanoparticles containing: cationic lipid (5 µM, 7.5 µM, 10 µM, 15 µM); cationic lipid (5 µM, 7.5 µM, 10 µM, 15 µM) & Curcumin (2.5 µM, 5 µM, 7.5 µM, 10 µM); cationic lipid (5 µM, 7.5 µM, 10 µM, 15 µM) & PTX (5 nM, 7.5 nM, 10 nM, 20 nM) and cationic lipid (5 µM, 7.5 µM, 10 µM, 15 µM), PTX (5 nM, 7.5 nM, 10 nM, 20 nM) & Curcumin (1.25 µM, 2.5 µM, 3.75 µM, 5 µM) for 24 h. Cellular cytotoxicities of drugs encapsulated in lipid nanoparticles were measured by MTT assay.

cytotoxicity was observed in killing non-cancerous cells (Figure 4e-f) treated with 16-GH+Cur+PTX.

Flow Cytometric apoptosis analysis

Next, we evaluated the conventional Annexin V/Propidium iodide (PI) binding based flow cytometric assay to examine apoptosis inducing efficiency of lipid nanoparticles quantitatively. CT-26 cells treated with nanoparticles of lipid 16-GH+Cur+PTX significantly enhanced accumulation of late apoptotic cells compared to nanoparticles of lipid 16-GH, nanoparticles of lipid 16-GH+Cur and nanoparticles of lipid 16-GH+PTX (Figure 5). Thus, the results clearly demonstrated that the lipid nanoparticles were efficient in inducing apoptosis in cancer cells.

BrdU incorporation assay

Next, we evaluated the relative efficiencies of lipid nanoparticles in inhibiting proliferations of CT-26 and NIH3T3 cells. BrdU (5-bromo-2-deoxyuridine) incorporation assay was used for detecting BrdU incorporated cells, i.e. for detecting actively replicating cells. When cells are cultured with labeling medium that contains BrdU, this pyrimidine analog is incorporated in place of thymidine into the newly synthesized DNA of proliferating cells. After removing labeling medium, cells are fixed and the DNA is denatured with our fixing/denaturing solution. Then a BrdU mouse mAb is added to detect the incorporated BrdU (The denaturing of DNA is necessary to improve the accessibility of the incorporated BrdU to the detection antibody). Anti-mouse IgG, HRP-linked antibody is then used to recognize the bound detection antibody. HRP substrate TMB is added to develop color. The magnitude of the absorbance for the developed color

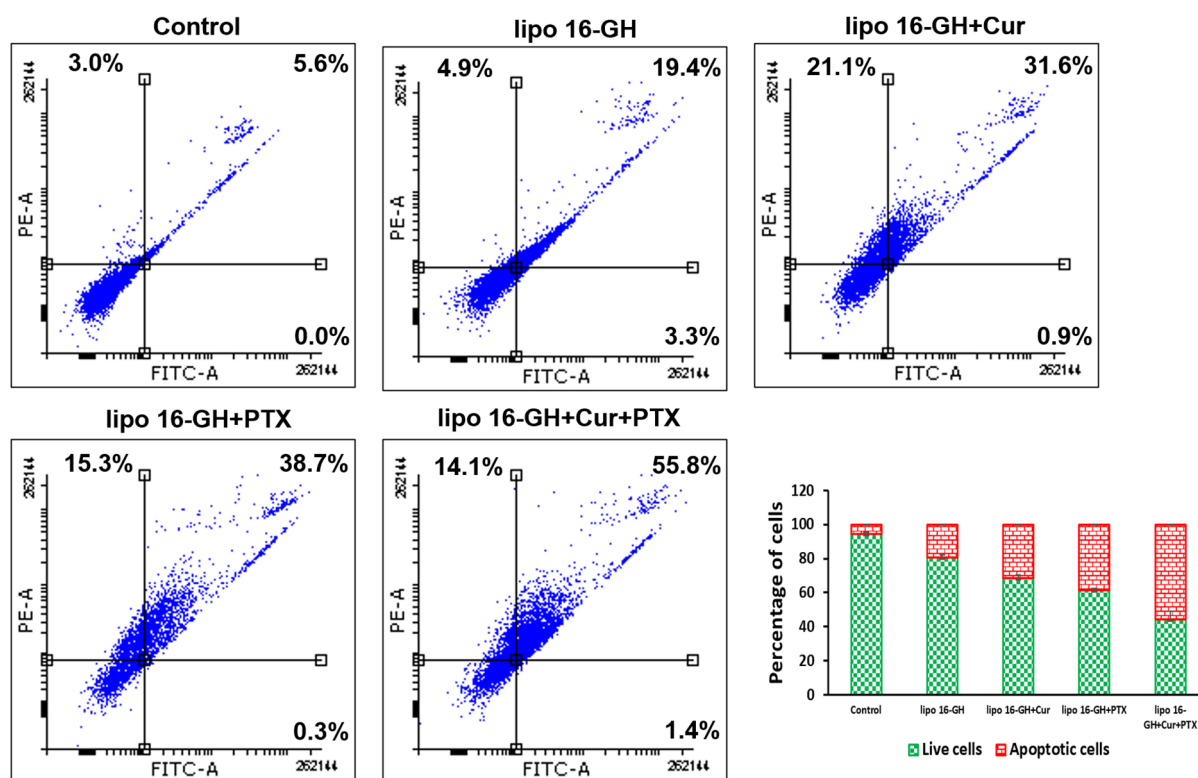


Figure 5. Lipid nanoparticles encapsulated with Curcumin & PTX induces significant apoptosis in CT-26 cells. CT-26 cells were treated with: nanoparticles containing 15 μ M lipid 16-GH without any drug, nanoparticles containing 15 μ M lipid 16-GH & 10 μ M Curcumin; nanoparticles containing 15 μ M lipid 16-GH & 20 nM PTX; and nanoparticles containing 10 μ M lipid 16-GH & 5 μ M Curcumin & 10 nM PTX. Both untreated and treated cells were stained with FITCAnnexin V and propidium iodide (PI) for flow cytometric analysis. The horizontal and vertical axes represent cells labeled with FITC-Annexin V and PI, respectively in the dot plot. Dots in the upper right quadrant represent late apoptotic cells (positive for both Annexin V and PI).

is proportional to the quantity of BrdU incorporated into cells, which is a direct indication of cell proliferation. Findings in the BrdU incorporation assay (**Figure 6a**) clearly revealed that lipid nanoparticles containing both Curcumin & PTX exhibit more effective anti-proliferative properties in tumor CT-26 cells but not in NIH3T3.

Cell cycle arrest study

To explore the mechanisms of exerted inhibition of tumor cell growth by the presently described lipid nanoparticles, CT-26 cells were treated with lipid nanoparticles for 24 h, estimated the cyclin B1 content (marker for G2/M phase of cell cycle) by the flow cytometry. Cells treated with nanoparticles of lipid 16-GH+Cur+PTX showed enhanced populations of cells arrested in G2/M-phase compared to G2/M populations of cells treated with other lipid nanoparticles (**Figure 6b-e**). PTX, which belongs to taxane family, is a highly effective anti-cancer drug that effectively binds to microtubule and stabilizes microtubule structure [23]. Thus, mitotic spindle dynamics is suppressed leading to cell cycle arrest at G2/M phase and induction of apoptosis [24]. Studies in a variety of cell lines have demonstrated that Curcumin exerts antiproliferative effects by inducing not only apoptosis but also cell cycle arrest [25]. Thus, the cell growth inhibition efficacy of presently described nanoparticles of lipid 16-GH+Cur+PTX may originated from enhanced efficacies of combined drug

formulations in arresting tumor cells at the G2/M phase of cell cycle.

Effect on mitochondrial membrane depolarization

Mitochondrial membrane potential ($\Delta\Psi_m$) is an important variable of mitochondrial role and can be used to distinguish apoptotic and viable cells [20]. Healthy cells normally have less $\Delta\Psi_m$ than tumor cells. During apoptosis, several crucial events take place in mitochondria. Cationic JC-1 dye, which is membrane permeable and reversibly changes color from red (high membrane potential) to green (low membrane potential, depolarization). In viable cancer cells, due to the greater $\Delta\Psi_m$, JC-1 forms J-aggregates (complexes) with strong red fluorescence at 600 nm. Contrastingly, in apoptotic cells due to low $\Delta\Psi_m$, JC-1 exists in the monomeric form, with green fluorescence at 525 nm [26, 27]. In the present study, CT-26 cells were incubated with lipid nanoparticles at 2 μ M for 4 h and then medium was added with JC-1 dye and incubated at 37 $^{\circ}$ C for 1h in dark. Next, fluorescence emission shift from red to green was analyzed using flow cytometer. The percentage of cell population consisting polarized (high $\Delta\Psi_m$) or depolarized mitochondria (low $\Delta\Psi_m$) were shown in **Figure 8**. Importantly, the percentage of apoptotic cells with depolarized mitochondria were drastically increased in cells treated with nanoparticles of lipid 16-GH+Cur+PTX compared to control treated cells. The

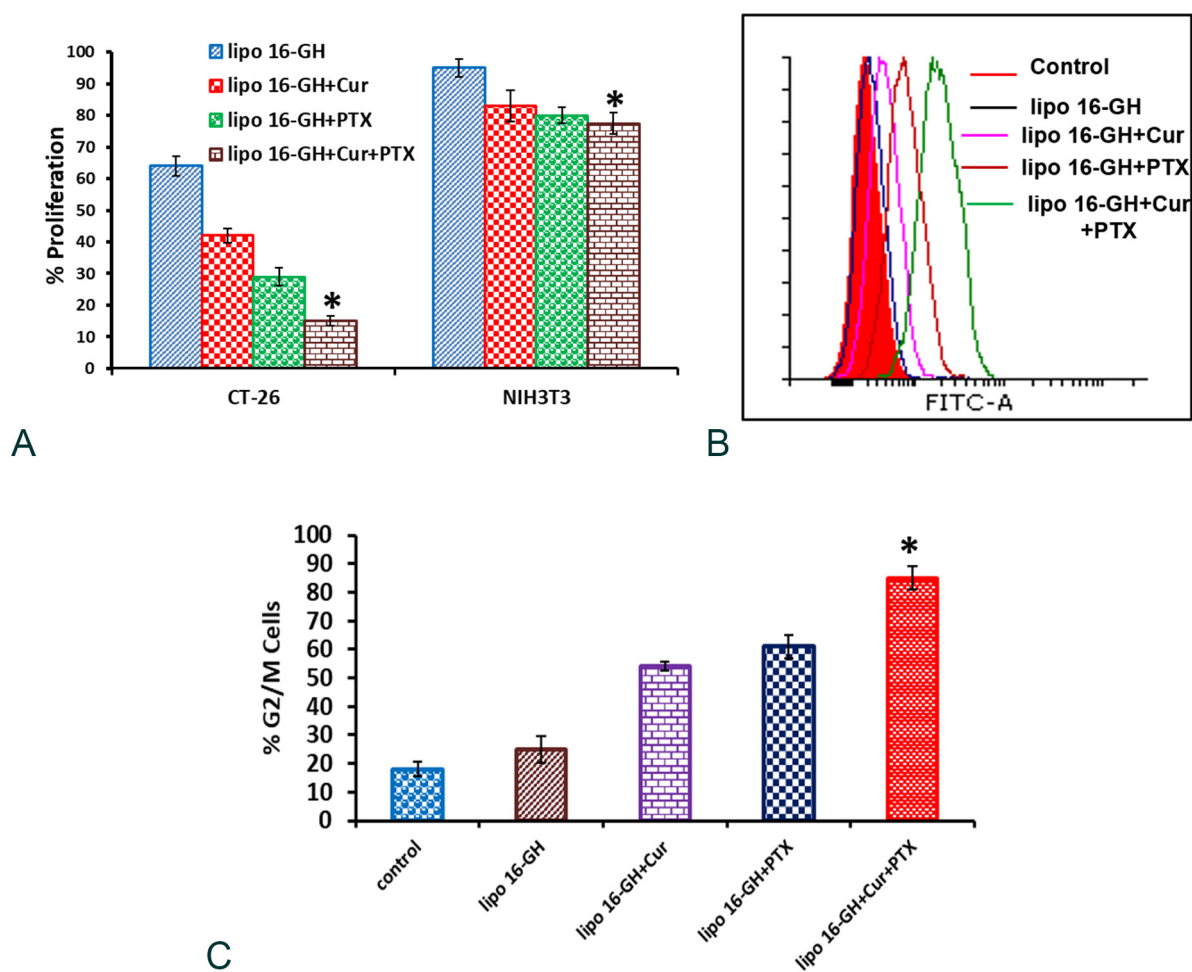


Figure 6. Lipid nanoparticles containing Curcumin & PTX significantly inhibited proliferation and enhanced population of cells arrested in G2/M phase. (a) Proliferation behaviors of various lipid nanoparticles in CT-26 and NIH3T3 cells were measured by the BrdU incorporation assay (* $P < 0.05$ vs. lipo 16-GH+PTX). (b) CT-26 cells were treated with lipid nanoparticles. Both treated and untreated cells were trypsinized, fixed, permeabilized, incubated with primary antibody of cyclin B1 (a marker of G2/M phase) followed by incubation with (FITC) conjugated secondary antibody and finally analyzed by flow cytometry. Overlap of FACS profiles for the cyclin B1 for cell treated with: nanoparticles of lipid 16-GH (blue); nanoparticles of lipid 16-GH+Cur (green); nanoparticles of lipid 16-GH+PTX (violet); nanoparticles of lipid 16-GH+Cur+PTX (pink) and untreated cells (black). (c) Graphical representation of % of cells in G2/M phase (* $P < 0.05$ vs lipo 16-GH+PTX).

results summarized in **Figure 7** confirm that nanoparticles of lipid 16-GH+Cur+PTX are efficient in initiating apoptosis by collapsing the $\Delta\Psi_m$ in tumor cells.

Effect on caspase-3 and caspase-9

Initiation of cellular events of apoptosis is mainly mediated by cysteine protease (thiol proteases) family enzymes known as caspases [28]. In the present study, the activities of caspase-3 and -9 were evaluated using LEHD-pNA and Ac-DEVD-pNA substrates, which are cleaved by caspase-3 and caspase-9, respectively. Interestingly, nanoparticles of lipid 16-GH+Cur+PTX significantly increased levels of caspase-3 and caspase-9 compared to nanoparticles of lipid 16-GH+Cur or nanoparticles of lipid 16-GH+PTX incubated cells. Cells incubated with nanoparticles of lipid 16-GH+Cur+PTX for 24 h displayed significantly greater caspase-3 ($0.98 \pm 0.4 \mu\text{M pNA/mg protein/min}$) and caspase-9

($0.91 \pm 0.1 \mu\text{M pNA/mg protein/min}$) activity. Contrastingly, the activities of caspase-3 and -9 (**Figure 8**) were decreased when pre-incubated for 1 h with caspase inhibitors.

Conclusion

Encapsulation of Curcumin and PTX in lipid nanoparticles of pH-sensitive histidinylated cationic amphiphile were prepared and assigned for therapy on various cancer cells in vitro. The obtained lipid nanoparticles inhibited the growth of cancer cells in vitro through increasing cell cycle arrest in G2/M phase, apoptosis induction and cellular uptake. Further, in depth mechanistic investigations need to be performed in the future toward obtaining clear mechanistic insights on the cancer cell specific cytotoxic nature of the presently described lipid nanoparticles of histidinylated cationic amphiphile. Thus, the lipid nanoparticles described herein have potential use as efficient tumor cell

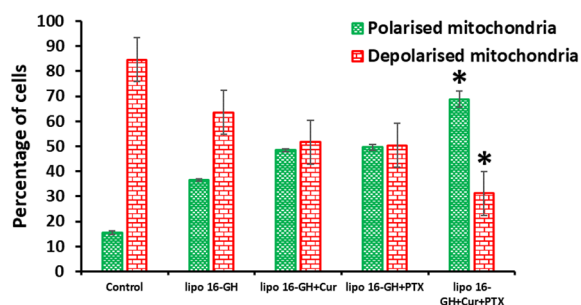


Figure 7. Mitochondrial membrane depolarization ($\Delta\Psi_m$) analysis by JC-1 stained CT-26 cells treated with lipid nanoparticles for 2 h. Percent of cells with depolarized or polarized mitochondria based on the scatter plots (* $P < 0.005$ vs. lipo 16-GH+PTX).

inhibitors and may have therapeutic implications against various cancers.

Acknowledgements

We thank Director, CSIR-IICT, Hyderabad for providing facilities throughout the study.

Author contributions

GKM designed the study and SV carried out the experiments and prepared the first draft of the manuscript. GKM coordinated the study and finalized the manuscript.

Competing interests

All authors disclose no competing interests.

References

- Ge Z, Liu S. Functional block copolymer assemblies responsive to tumor and intracellular microenvironments for site-specific drug delivery and enhanced imaging performance. *Chem Soc Rev* 2013; 42 (17): 7289-7325.
- Torchilin VP. Multifunctional, stimuli-sensitive nanoparticulate systems for drug delivery. *Nat Rev Drug Discov* 2014; 13 (11): 813-827.
- Gurman P, Miranda OR, Clayton K, Rosen Y, Elman NM. Clinical Applications of Biomedical Microdevices for Controlled Drug Delivery. *Mayo Clin Proc* 2015; 90 (1): 93-108.
- Eguchi H, Umemura M, Kurotani R, Fukumura H, Sato I, Kim JHA et al. A magnetic anti-cancer compound for magnet-guided delivery and magnetic resonance imaging. *Sci Rep* 2015; 17: 9194.
- Senapati S, Mahanta AK, Kumar S. et al. Controlled drug delivery vehicles for cancer treatment and their performance. *Sig Transduct Target Ther* 2018; 3: 7.
- Chen Y, Yang C, Mao J, Li H, Ding J, Zhou W. Spermine modified polymeric micelles with pH-sensitive drug release for targeted and enhanced antitumor therapy. *RSC Adv* 2019; 9: 11026-11037.

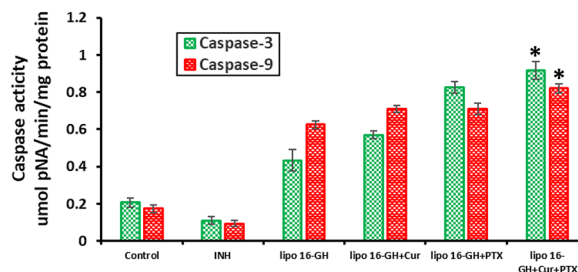


Figure 8. Effect of various lipid nanoparticles on the expression levels of caspase-3/9 in the presence or absence of 20 μ M caspase inhibitors for 24 h were analysed using spectrophotometer (* $P < 0.05$ vs. lipo 16-GH+PTX).

- Rashidzadeh H, Rezaei SJT, Zamani S, Sarijloo E, Ramazani A. pH-sensitive Curcumin conjugated micelles for tumor triggered drug delivery. *J Biomater Sci Polym Ed* 2021; 32 (3): 320-336.
- Moku G, Gulla SK, Nimmu NV, Khalid S, Chaudhuri A. Delivering anti-cancer drugs with endosomal pH-sensitive anti-cancer liposomes. *Biomater Sci* 2016; 4 (4): 627-638.
- Zhang L, Wang Y, Yang Y, Liu Y, Ruan S, Zhang Q. High Tumor Penetration of Paclitaxel Loaded pH Sensitive Cleavable Liposomes by Depletion of Tumor Collagen I in Breast Cancer. *ACS Appl Mater Interfaces* 2015; 7 (18): 9691-9701.
- Cheng CJ, Bahal R, Babar IA, Pincus Z, Barrera F, Liu C, Svoronos A, Braddock DT, Glazer PM, Engelman DM, Saltzman WM, Slack FJ. MicroRNA silencing for cancer therapy targeted to the tumour microenvironment. *Nature* 2015; 518(7537): 107-110.
- Du JZ, Du XJ, Mao CQ, Wang J. Tailor-made dual pH-sensitive polymer-doxorubicin nanoparticles for efficient anticancer drug delivery. *J Am Chem Soc* 2011; 133 (44): 17560-17563.
- Kaur S, Prasad C, Balakrishnan B, Banerjee R. Trigger responsive polymeric nanocarriers for cancer therapy. *Biomater Sci* 2015; 3 (7): 955-987.
- Kim BJ, Cheong H, Hwang BH, Cha HJ. Mussel-inspired protein nanoparticles containing Iron (III)-DOPA complexes for pH-responsive drug delivery. *Angew Chem Int Ed Engl*. 2015; 54 (25): 7318-7322.
- Liu J, Huang Y, Kumar A, Tan A, Jin S, Mozhi A, Liang XJ. pH-sensitive nano-systems for drug delivery in cancer therapy. *Biotechnol Adv* 2014; 32 (4): 693-710.
- James J, Langer R, Chen J. A Novel Mechanism is involved in cationic lipid-mediated functional siRNA delivery. *Mol Pharma* 2009; 6 (3): 763-771.
- Jia L, Yu G, Zhang Y, Wang MM. Lysosome-dependent degradation of Notch3. *Int J Biochem Cell Biol* 2009; 41 (12): 2594-2598.
- D. Collins, D. In *Liposomes as Tools in Basic Research and Industry* (Philippot, J. R. and Schuber, F., eds, CRC Press, Inc., Boca Raton, FL) 1995; 201.
- Budker V, Gurevich V, Hagstrom JE, Bortzov F, Wolff JA. pH-sensitive, cationic liposomes: a new synthetic virus-like vector. *Nat Biotechnol* 1996; 14 (6): 760-764.
- Remy JS, Goula D, Steffan AM, Zanta MA, Bousiff O, Behr JP, Demenx B, Kabanov AV, Felgner PL, Seymour L. Editors, England: John Wiley & Sons, 1998.

20. Garu A, Moku G, Gulla SK, Pramanik D, Majeti BK, Karmali PP, Shaik H, Sreedhar B, Chaudhuri A. Examples of Tumor Growth Inhibition Properties of Liposomal Formulations of pH-Sensitive Histidinylated Cationic Amphiphiles. *ACS Biomater Sci Eng* 2015; 1(8): 646-655.
21. Kumar VV, Pichon C, Refregiers M, Guerin B, Midoux P, Chaudhuri A. Single histidine residue in head-group region is sufficient to impart remarkable gene transfection properties to cationic lipids: evidence for histidine-mediated membrane fusion at acidic pH. *Gene Ther* 2003; 10 (15): 1206-1215.
22. Bisht S, Feldmann G, Soni S, Ravi R, Karikar C, Maitra A, Maitra A. Polymeric nanoparticle-encapsulated Curcumin ("nanoCurcumin"): a novel strategy for human cancer therapy. *J Nanobiotechnology* 2007; 5: 3.
23. McGrogan BT, Gilmartin B, Carney DN, McCann A. Taxanes, microtubules and chemoresistant breast cancer. *Biochim Biophys Acta* 2008; 1785 (2): 96-132.
24. Xiao H, Verdier-Pinard P, Fernandez-Fuentes N, Burd B, Angeletti R, Fiser A, Horwitz SB, Orr GA. Insights into the mechanism of microtubule stabilization by Taxol. *Proc Natl Acad Sci USA* 2006; 103 (27): 10166-10173.
25. Lin SS, Huang HP, Yang JS, Wu JY, Hsia TC, Lin CC, Lin CW, Kuo CL, Gibson Wood W, Chung JG. DNA damage and endoplasmic reticulum stress mediated Curcumin-induced cell cycle arrest and apoptosis in human lung carcinoma A-549 cells through the activation caspases cascade- and mitochondrial-dependent pathway. *Cancer Lett* 2008; 272 (1): 77-90.
26. Sharpe JC, Arnoult D, Youle RJ. Control of mitochondrial permeability by Bcl-2 family members. *Biochim Biophys Acta* 2004; 1644 (2-3): 107-113.
27. Yang WL, Addona T, Nair DG, Qi L, Ravikumar TS. Apoptosis induced by cryo-injury in human colorectal cancer cells is associated with mitochondrial dysfunction. *Int J Cancer* 2003; 103 (3): 360-369.
28. Li P, Nijhawan D, Budihardjo I, Srinivasula SM, Ahmad M, Alnemri ES, Wang X. Cytochrome c and dATP-dependent formation of Apaf-1/caspase-9 complex initiates an apoptotic protease cascade. *Cell* 1997; 91 (4): 479-489.